Development 136, 1453-1464 (2009) doi:10.1242/dev.034967

Foxg1 promotes olfactory neurogenesis by antagonizing *Gdf11*

Shimako Kawauchi[1,*], Joon Kim[1,*,†], Rosaysela Santos[1], Hsiao-Huei Wu[1,‡], Arthur D. Lander[2] and Anne L. Calof[1,§]

Foxg1, a winged-helix transcription factor, promotes the development of anterior neural structures; in mice lacking *Foxg1*, development of the cerebral hemispheres and olfactory epithelium (OE) is severely reduced. It has been suggested that *Foxg1* acts by positively regulating the expression of growth factors, such as Fgf8, which support neurogenesis. However, Foxg1 also binds Smad transcriptional complexes, allowing it to negatively regulate the effects of TGFβ family ligands. Here, we provide evidence that this latter effect explains much of the ability of Foxg1 to drive neurogenesis in the OE. We show that *Foxg1* is expressed in developing OE at the same time as the gene encoding growth differentiation factor 11 (Gdf11), a TGFβ family member that mediates negative-feedback control of OE neurogenesis. Mutations in *Gdf11* rescue, to a considerable degree, the major defects in *Foxg1*$^{-/-}$ OE, including the early, severe loss of neural precursors and olfactory receptor neurons, and the subsequent collapse of both neurogenesis and nasal cavity formation. Rescue is gene-dosage dependent, with loss of even one allele of *Gdf11* restoring substantial neurogenesis. Notably, we find no evidence for a disruption of *Fgf8* expression in *Foxg1*$^{-/-}$ OE. However, we do observe both a failure of expression of follistatin (*Fst*), which encodes a secreted Gdf11 antagonist normally expressed in and around OE, and an increase in the expression of *Gdf11* itself within the remaining OE in these mutants. *Fst* expression is rescued in *Foxg1*$^{-/-}$*;Gdf11*$^{-/-}$ and *Foxg1*$^{-/-}$*;Gdf11*$^{+/-}$ mice. These data suggest that the influence of Foxg1 on Gdf11-mediated negative feedback of neurogenesis may be both direct and indirect. In addition, defects in development of the cerebral hemispheres in *Foxg1*$^{-/-}$ mice are not rescued by mutations in *Gdf11*, nor is *Gdf11* expressed at high levels within these structures. Thus, the pro-neurogenic effects of *Foxg1* are likely to be mediated through different signaling pathways in different parts of the nervous system.

KEY WORDS: Mouse, Olfactory epithelium, TGFβ, Follistatin, p21Cip1, Fgf8, Neuronal progenitor, Neurogenesis, Mash1, Ngn1, Sox2, Olfactory receptor neuron, Cerebral cortex, Gene dosage

INTRODUCTION

Forkhead or Fox proteins comprise a large family of 'winged-helix' transcription factors that regulate diverse developmental processes in mammals (Carlsson and Mahlapuu, 2002). *Foxg1* is highly expressed in anterior neural structures, and promotes their development; neural structures whose development is adversely affected in *Foxg1*$^{-/-}$ mice include the cerebral cortex, ventral telencephalon, ear, retina and olfactory epithelium (OE) (Duggan et al., 2008; Hanashima et al., 2007; Hanashima et al., 2004; Hebert and McConnell, 2000; Martynoga et al., 2005; Pauley et al., 2006; Pratt et al., 2004; Xuan et al., 1995). In mice that are null for *Foxg1*, the cerebral hemispheres are dramatically reduced in size, ventral telencephalic structures are lacking, and the animals die at birth (Xuan et al., 1995). *Foxg1* is also expressed in the OE from an early age (Hatini et al., 1999), and *Foxg1*$^{-/-}$ mice lack an OE and most of the nasal cavity (Xuan et al., 1995). For these reasons, Foxg1 has been described as a general positive regulator of anterior nervous system development.

It has been proposed that positive effects of Foxg1 on neurogenesis are closely linked to the effects of fibroblast growth factors (FGFs) (reviewed by Hebert and Fishell, 2008). In the telencephalon, *Foxg1* positively regulates expression of *Fgf8* (Martynoga et al., 2005), which plays a central role in neurogenesis not only in the telencephalon, but also in the OE (Kawauchi et al., 2005). Although these data raise the possibility that Foxg1 promotes neurogenesis by inducing *Fgf8*, other studies indicate that FGFs such as FGF8 act upstream of *Foxg1* to control Foxg1 expression and function (Regad et al., 2007; Shimamura and Rubenstein, 1997; Storm et al., 2006).

An alternative mechanism by which Foxg1 could influence neural development is through its effects on the transforming growth factor beta (TGFβ) pathway (Dou et al., 2000; Rodriguez et al., 2001; Seoane et al., 2004). TGFβ family ligands signal primarily by triggering the phosphorylation of receptor-regulated Smads, which translocate to the nucleus and interact with diverse DNA-binding proteins to influence the transcription of target genes (Massague, 2000; Moustakas et al., 2001). Experiments using cultured neuroepithelial cells and cell lines have demonstrated that, upon treatment with TGFβ1, Foxg1 binds to a Smad3-containing complex and prevents it from inducing the expression of *p21Cip1* (*Cdkn1a* – Mouse Genome Informatics), which encodes a cyclin-dependent kinase inhibitor (CKI) that is both a Smad3 target gene and an effector of TGFβ-mediated cell cycle arrest (Dou et al., 2000; Massague and Gomis, 2006; Rodriguez et al., 2001; Seoane et al., 2004). These findings indicate that, in cells that express Foxg1, Foxg1 can interact directly with Smad-containing transcriptional complexes to block the expression of TGFβ target genes.

Recently, we discovered that growth differentiation factor 11 (Gdf11), a member of the TGFβ superfamily, is an important component of an autocrine negative-feedback loop that regulates neurogenesis in the OE (Kawauchi et al., 2004; Kawauchi et al., 2005; Wu et al., 2003). *Gdf11* is made by olfactory receptor neurons

[1]Department of Anatomy and Neurobiology and the Center for Complex Biological Systems, University of California, Irvine, CA 92697, USA. [2]Department of Developmental and Cell Biology and the Center for Complex Biological Systems, University of California, Irvine, CA 92697, USA.

*These authors contributed equally to this work
[†]Present address: Department of Neurosciences, University of California, San Diego, La Jolla, CA 92093, USA
[‡]Present address: Vanderbilt Center for Stem Cell Biology, Vanderbilt University, Nashville, TN 37232, USA
[§]Author for correspondence (e-mail: alcalof@uci.edu)

Accepted 17 February 2009

(ORNs) and late-stage neuronal progenitors (immediate neuronal precursors, or INPs) within the OE proper, and is present there as early as embryonic day 10.5 (E10.5) (Nakashima et al., 1999; Wu et al., 2003) (also see Results). Tissue culture studies show that Gdf11 can both arrest the division of INPs and promote the differentiation of INP progeny, effects that are accompanied by increased expression of the CKI p27Kip1 (Lander et al., 2009; Wu et al., 2003). Moreover, *Gdf11*-null mice show increased OE neurogenesis in vivo, with increased numbers of proliferating INPs and an extra layer of ORNs (Wu et al., 2003).

As a member of the activin branch of the TGFβ superfamily (Nakashima et al., 1999; Newfeld et al., 1999; Schneyer et al., 2008), Gdf11 signals via the same receptor-activated Smads (Smad2 and Smad3) as Tgfβ1 (Nomura et al., 2008; Tsuchida et al., 2007). This raises the possibility that some of the effects of Foxg1 on neurogenesis in the OE are due to antagonism of Gdf11 signaling. To test this, we analyzed OE development in *Foxg1;Gdf11* compound mutant mice. We observed that deficits in neurogenesis in the $Foxg1^{-/-}$ OE, which are apparent from the earliest times in OE development, are substantially rescued in $Foxg1^{-/-};Gdf11^{-/-}$ mice, and even in $Foxg1^{-/-};Gdf11^{+/-}$ mice. Alterations in the expression of follistatin (*Fst*), which encodes a secreted Gdf11 antagonist, appear to account for part of this rescue. Overall, our results imply that the pro-neurogenic effects of *Foxg1* in the OE are mediated, to a large degree, by antagonism of *Gdf11*. Interestingly, analysis of the same animals indicates that, in the cerebral cortex, *Foxg1* acts through different targets.

MATERIALS AND METHODS

Animals

$Gdf11^{-/-}$ mice ($Gdf11^{tm2/tm2}$; $Gdf11^{+/tm2}$ is the second of two reported null alleles) (Wu et al., 2003) were obtained by intercrossing $Gdf11^{+/tm2}$ mice maintained on a C57bl/6J background (Jackson Labs, Bar Harbor, ME, USA). $Foxg1^{cre/+}$ mice, in which the *Foxg1* coding sequence is replaced by the gene encoding Cre-recombinase (*Cre*) (Hebert and McConnell, 2000), were maintained on an outbred Swiss Webster background (Harlan, Indianapolis, IN, USA). Although expression of Cre recombinase in the *Foxg1* locus has been shown to have some effects on telencephalon development when the allele is maintained on a congenic C57bl/6 background (Eagleson et al., 2007), when maintained on an outbred background, $Foxg1^{cre/cre}$ mice have been shown to have nervous system phenotypes identical to those observed in another *Foxg1* null strain, $Foxg1^{lacZ/lacZ}$ (Duggan et al., 2008; Eagleson et al., 2007; Hanashima et al., 2007; Martynoga et al., 2005; Muzio and Mallamaci, 2005; Pratt et al., 2004). Therefore, we used $Foxg1^{cre}$ as a null allele and $Foxg1^{cre/cre}$ mice are designated $Foxg1^{-/-}$ hereafter. $Foxg1^{+/-};Gdf11^{+/-}$ mice were obtained by crossing $Gdf11^{+/-}$ females with $Foxg1^{+/-}$ male animals. Double knockouts ($Foxg1^{-/-};Gdf11^{-/-}$) and compound mutants ($Foxg^{-/-};Gdf11^{+/-}$) were obtained by intercrossing the resulting $Foxg1^{+/-};Gdf11^{+/-}$ mice. Mid-day of the day of vaginal plug detection was designated embryonic day 0.5 (E0.5). All protocols for animal use were approved by the Institutional Animal Care and Use Committee of the University of California, Irvine.

Tissue culture, in situ hybridization, immunofluorescence, histology and TUNEL staining

Dissected tissues were fixed, cryoprotected, embedded and cryosectioned (12-20 μm) as described (Murray et al., 2003). Hematoxylin staining was performed using Mayer's Hematoxylin solution (Sigma MHS 16-500, St Louis, MO, USA). In situ hybridization (ISH) was performed according to published protocols (Murray et al., 2003). cRNA probes used in this study were generated from: 1.5 kb mouse *Foxg1* partial cDNA (Calof et al., 2002); 1.2 kb mouse *Gdf11* partial cDNA (Wu et al., 2003); 1.0 kb mouse follistatin full-length cDNA (generous gift of M. M. Matzuk, Baylor College of Medicine, Houston, TX, USA); 0.6 kb mouse *Sox2* partial cDNA (Kawauchi et al., 2004); 2.0 kb mouse *Mash1* full-length cDNA (Guillemot and Joyner, 1993); 2.0 kb mouse *Ngn1* cDNA (Ma et al., 1999); 391 bp mouse *Ncam* cDNA (Barthels et al., 1987); 687 bp mouse *Otx2* partial cDNA (bp 894-1581 of GenBank accession number NM144841); full-length mouse *Fgf8* ORF (Kawauchi et al., 2005); full-length of P1 bacteriophage Cre recombinase cDNA (Lewandoski et al., 1997); 675 bp mouse *p21Cip1* cDNA (bp 380-1055 of GenBank accession number NM007669).

For pulse-fix analysis of bromodeoxyuridine (BrdU) incorporation, BrdU (Sigma) was injected intraperitoneally into pregnant dams (50 μg/gm body weight) and embryos collected 30 minutes later. Tissue (12 μm cryosections) was processed for anti-BrdU immunoreactivity as described (Kawauchi et al., 2005; Kim et al., 2005). TUNEL (deoxynucleotidyl Transferase-mediated dUTP Nick End Label) staining to detect DNA fragmentation in apoptotic cells was performed as described (Kawauchi et al., 2005), except that 20 μm cryosections were used.

Explant cultures from E14.5-E15.5 CD-1 mice (Charles River, Wilmington, MA, USA) were prepared as described (DeHamer et al., 1994; Wu et al., 2003). Purified recombinant human GDF11 (20 ng/ml; obtained by agreement with Wyeth Pharmaceuticals, Cambridge, MA, USA) was added at the beginning of the culture period. After 14 hours in vitro, explants were fixed as described (Wu et al., 2003) and processed for p21Cip1 immunoreactivity using monoclonal mouse anti-p21Cip1 (1:1000;

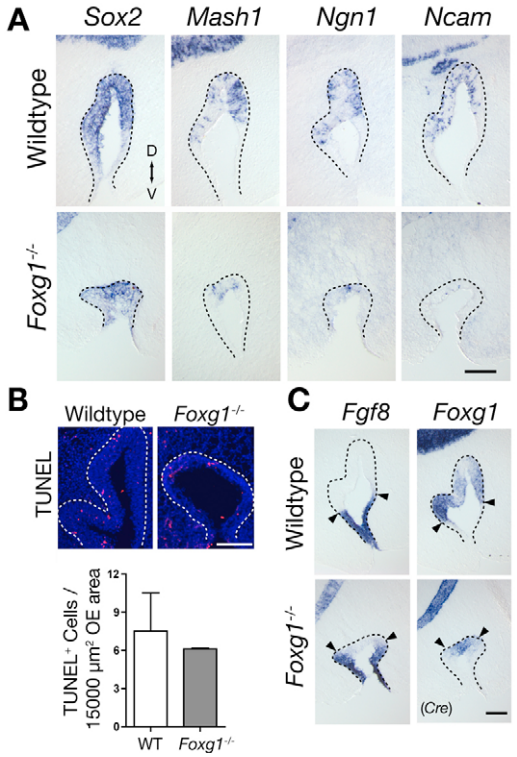

Fig. 1. Failure of primary neurogenesis in $Foxg1^{-/-}$ OE. (**A**) Sections of olfactory epithelium (OE) from wild-type and $Foxg1^{-/-}$ mouse embryos at E11, showing the decrease in the numbers of cells expressing stage-specific neuronal markers. D, dorsal; V, ventral. (**B**) Apoptotic cells visualized by TUNEL labeling in E11 OE from wild-type and $Foxg1^{-/-}$ OE. For comparison, numbers were normalized to an area of 15,000 μm^2, the average area of each section of $Foxg1^{-/-}$ OE at this age. Mean values ±s.d. of TUNEL$^+$ cells per 15,000 μm^2 OE are: wild type, 7.51±4.24; $Foxg1^{-/-}$, 6.11±0.095. Data, which showed no significant difference (Student's *t*-test) (Glantz, 2005), were collected from two animals of each genotype. (**C**) *Fgf8* and *Foxg1* expression at E11. *Fgf8* is expressed at the rim of the olfactory pit (OP) in wild type, and the pattern is unchanged in $Foxg1^{-/-}$ OE (arrowheads). The *Foxg1* expression domain (detected by ISH to *Cre*), located in the central neurogenic zone of the OE, is reduced in $Foxg1^{-/-}$ OE. Scale bars: 100 μm.

Neomarker, Fremont, CA, USA: clone # AB-6 [HJ-21]), detected with unlabeled goat anti-mouse IgG (1:300; Southern Biotech, Birmingham, AL, USA), followed by Cy2-conjugated donkey anti-goat-IgG (1:100; Jackson ImmunoResearch, West Grove, PA, USA). Cell nuclei were counterstained with Hoechst 33342 (10 μg/ml, Sigma). For quantification, total migratory cells in a minimum number of 10 randomly chosen fields were counted for each condition (n=500-1000 cells per condition). The mean fluorescence intensity for each cell was quantified as the mean pixel density over the total area of the cell, measured using Zeiss AxioVision software (Carl Zeiss, Thornwood, NY, USA). The percentage of cells with mean fluorescence intensities of >6500 ('P21+ cells') was plotted for each condition (mean fluorescence intensity for >95% of cells in both control and no-first-antibody conditions was <6500).

Quantitative RT-PCR

Total RNA (4 μg) was isolated from OE turbinates (E16.5) or frontonasal processes (E11.5; OE and underlying mesenchyme, excluding forebrain) for each of 2-3 embryos of the indicated genotypes. Aurum Total RNA Mini Kit (BioRad, Hercules, CA, USA) was used for RNA isolation, and RNA was reverse transcribed using Superscript III reverse transcriptase and random oligonucleotide hexamers (Invitrogen, Carlsbad, CA, USA). Reactions were assembled using iQ SYBR Green Supermix (BioRad). Specificity of amplification was verified for each reaction by examination of the corresponding melt curve. Normalization of *Gdf11* or *Sox2* transcripts was carried out using *Gapdh* (run in parallel reactions for all samples) to control for the amount of tissue in each sample (Nguyen et al., 2005). Possible artefacts from amplification of genomic DNA were controlled for by processing samples prepared without reverse transcriptase; in all cases these proved negative. All PCR reactions were performed on an iQ5 iCycler (BioRad). Cycling conditions were 95°C for 3 minutes followed by 35 cycles of 95°C for 30 seconds, 58°C for 30 seconds and 72°C for 45 seconds. Primers used were: mouse *Gdf11 exon3* (final concentration 200 nM), 5′-CTAAGCGCTACAAGGCCAAC-3′ and 5′-AGCATGTTGATTGGGGACAT-3′; mouse *Sox2 3′UTR* (100 nM), 5′-AAGGGTTCTTGCTGGGTTTT-3′ and 5′-AGACCACGAAAACGGTCTTG-3′; mouse *Gapdh* (150 nM), 5′-TTCACCACCATGGAGAAGGC-3′ and 5′-GGCATGGACTGTGGTCATGA-3′. PCR product sizes were 151 bp, 150 bp and 237 bp, respectively.

Delta cycle time (dCT) values were obtained for each reaction by subtracting the CT value of *Gapdh* for that reaction from the CT value of the tested transcript (*Gdf11* or *Sox2*) run in parallel. Means and standard errors (s.e.m.) were calculated for dCTs obtained from duplicate or triplicate reactions for each biological sample. To obtain ddCT values, the mean dCT for a given transcript in wild type was subtracted from the mean dCT for that same transcript obtained from a given experimental sample. Fold-change relative to the wild-type value was calculated as $2^{-(ddCT)}$. Errors in fold-change were propagated from errors of dCT values, as the square root of the sum of the squares of the error (s.e.m.) for the dCT value of each transcript.

RESULTS

Aberrant primary neurogenesis in the OE of *Foxg1*$^{-/-}$ mice

To understand when and how deficits in nasal cavity morphogenesis and OE neurogenesis occur in *Foxg1*$^{-/-}$ mice, ISH was performed using neuronal lineage markers at E11, when the olfactory pit (OP) first begins to invaginate. Even at this early stage of OE development, sometimes referred to as primary neurogenesis (Kawauchi et al., 2005), cells at all stages of the OE neuronal lineage are evident (Fig. 1A) (Beites et al., 2005; Kawauchi et al., 2004): neural stem cells can be identified by expression of *Sox2*; early committed neuronal progenitors that derive from these cells express the proneural gene *Mash1* (*Ascl1* – Mouse Genome Informatics); cells of the next lineage stage – referred to as immediate neuronal precursors (INPs) – express neurogenin 1 (*Ngn1*; *Neurog1* – Mouse Genome Informatics); and differentiated ORNs that derive from INPs are identified by expression of *Ncam* (*Ncam1* – Mouse Genome Informatics).

In *Foxg1*$^{-/-}$ embryos at E11, cells expressing these lineage markers were present, but were greatly reduced in number (Fig. 1A). Even at this early age, OPs were greatly reduced in size; the domain of *Sox2*-expressing neural stem cells was correspondingly reduced compared with that of wild-type littermates. In addition, the concentric arrangement of gene expression domains in the OP, reflective of cells at different states of neuronal differentiation (Cau et al., 1997; Kawauchi et al., 2005), was altered in *Foxg1*$^{-/-}$ embryos. Although some cells in the dorsal recess of *Foxg1*$^{-/-}$ OPs do express neuronal markers, the number of these cells was dramatically reduced compared with wild type, even when the relative decrease in OP size of the mutant was taken into account: only a few *Mash1*$^{+}$ early progenitors could be detected in a restricted dorsomedial domain, and the decrease in *Ngn1*$^{+}$ INPs and *Ncam*$^{+}$ ORNs cells was even more dramatic. By contrast, wild-type OPs at this stage displayed a clear concentric arrangement of neuronal cells: *Mash1*-expressing progenitors were present near the rim, with *Ngn1*-expressing INPs and *Ncam*-expressing ORNs at progressively more central zones. To assess whether the deficits in *Foxg1*$^{-/-}$ OE

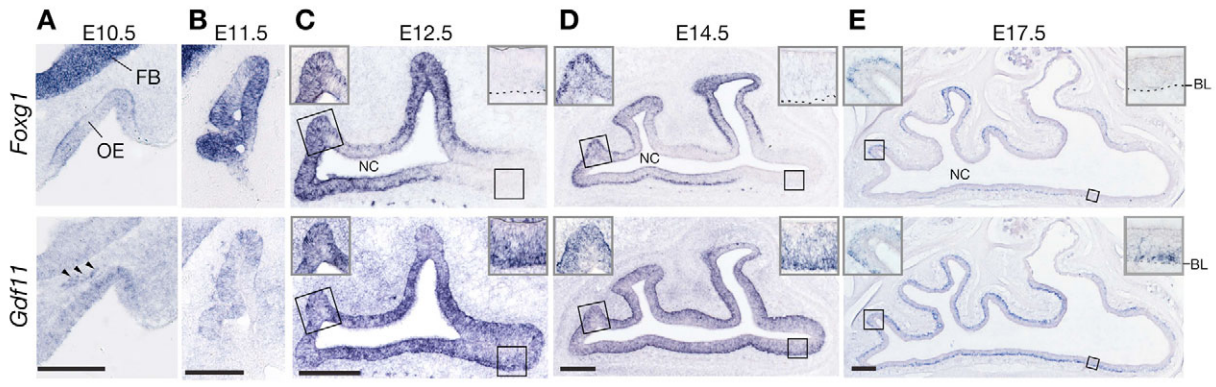

Fig. 2. Expression of *Foxg1* and *Gdf11* in developing mouse OE. (**A**,**B**) Coronal sections through heads of E10.5 and E11.5 wild-type mice. *Gdf11* expression is detected both in the OE and in a subset of cells in the mesenchyme, possibly migrating pioneer neurons (arrowheads). FB, forebrain; OE, olfactory epithelium. (**C-E**) Horizontal sections showing the OE in one-half of the nasal region (septum is at bottom) at E12.5, E14.5 and E17.5 in wild-type mice. The expression domains of *Foxg1* and *Gdf11* overlap, except in regions such as the anterior OE, which has ceased planar expansion at these ages. Insets show high magnification views of the OE at posterior regions of co-expression and anterior regions where co-expression has ceased (anterior is right; posterior, left). NC, nasal cavity; BL, basal lamina. Scale bars: 200 μm.

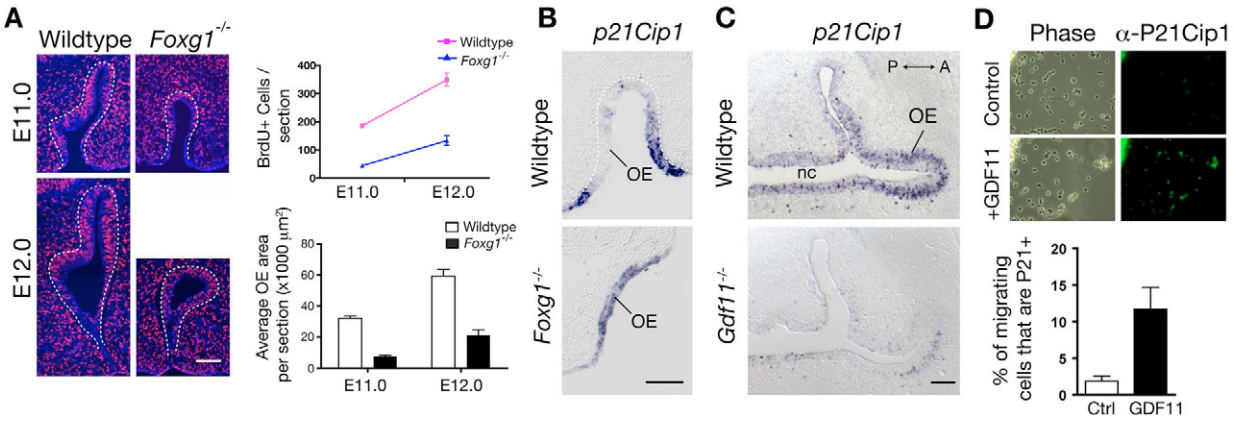

Fig. 3. Cell proliferation and p21Cip1 expression in mutant and wild-type OE. (**A**) BrdU pulse-fix experiments were performed as described in the Materials and methods, with pregnant dams injected at gestational day 11 or 12. Images show representative anti-BrdU immunostaining results. Graph shows quantification (mean±s.e.m.) of total number of BrdU$^+$ cells per OE section at each age in *Foxg1*$^{-/-}$ embryos (blue) and wild-type littermates (pink). Histogram shows average OE area per section for mutants versus wild types. The number of BrdU$^+$ cells is significantly lower in *Foxg1*$^{-/-}$ mutants at each age, as is the average area of OE per section (P<0.01, Student's t-test). Data were collected from two animals of each genotype at each age. (**B**) Coronal sections of an E10.5 *Foxg1*$^{-/-}$ embryo and a wild-type littermate, processed for ISH with a *p21Cip1* probe. Dorsal is up; ventral, down. OE, olfactory epithelium. Scale bar: 100 µm. (**C**) Horizontal sections of an E13.5 *Gdf11*$^{-/-}$ embryo and a wild-type littermate, processed as in B. nc, nasal cavity; A, anterior; P, posterior. Scale bar: 100 µm. (**D**, top) Immunofluorescence staining of migratory OE neuronal cells in explant cultures (after 14 hours in vitro), grown with or without Gdf11, then processed for anti-p21Cip1 immunoreactivity. (Bottom) Quantification of results from a typical culture experiment. Percentages of p21Cip1$^+$ cells were: 2.5% of 587 counted cells in control cultures; 14.3% of 1065 counted cells in GDF11-treated cultures. P<0.05, Student's t-test.

reflected an increase in cell death, TUNEL staining was performed. As shown in Fig. 1B, we found no significant difference in relative numbers or density of apoptotic cells in *Foxg1*$^{-/-}$ versus wild-type OE at E11. Together, these observations indicate that, in *Foxg1*$^{-/-}$ OE, development and differentiation of neuronal cells begins at the normal time. However, because there was no marked increase in apoptosis in *Foxg1* nulls, some other process must result in the markedly hypoplastic structure of *Foxg1*$^{-/-}$ OE.

Foxg1 is unlikely to act through regulation of *Fgf8* expression or signaling in the OE

In the telencephalon, *Foxg1* regulates the expression of *Fgf8*, and it has been proposed that morphological deficits due to loss of *Foxg1* may be explained in part by decreases in *Fgf8* expression (Martynoga et al., 2005). *Fgf8* is also essential for morphogenesis of the nasal cavity, and for neurogenesis within the OE (Kawauchi et al., 2005), but we saw no obvious change in *Fgf8* expression in the rim of *Foxg1*$^{-/-}$ OPs (Fig. 1C). In fact, the size of the *Fgf8*-expression domain appeared to be essentially normal in *Foxg1* mutants, despite a radical difference in OP size (Fig. 1C). We next compared the patterns of expression of *Fgf8* and *Foxg1* in the OPs of wild-type and *Foxg1* mutant embryos, in the latter case using a probe for *Cre* to detect cells with endogenous *Foxg1* promoter activity (see Materials and methods). In both wild-type and mutant embryos, we observed no overlap between the expression domains of *Foxg1* and *Fgf8* (Fig. 1C), which provides a probable explanation for the lack of a direct transcriptional relationship.

Although these data do not rule out the possibility that *Foxg1* acts by influencing *Fgf8* signaling, rather than *Fgf8* expression, this too seems unlikely given that we observe no increase in apoptosis in the *Foxg1*$^{-/-}$ OE (see above and Fig. 1B), whereas a marked increase in apoptosis of *Fgf8*$^+$/*Sox2*$^+$ primary neural stem cells is a hallmark phenotype when *Fgf8* is inactivated in and around the OE (Kawauchi et al., 2005). We thus infer that the disruption of nasal cavity morphogenesis and OE histogenesis (neurogenesis) in the *Foxg1* mutant is likely to occur through a mechanism that is distinct from a disruption in *Fgf8* expression and/or signaling.

Expression of *Gdf11* and *Foxg1* overlap in developing OE

As the first step toward testing the hypothesis that Foxg1 promotes neurogenesis via antagonism of Gdf11 signaling, we examined whether *Foxg1* and *Gdf11* are expressed at appropriate times and locations to interact in this way. At E10.5, widespread expression of *Foxg1* mRNA was observed in the neuroepithelium of the invaginating OP, as well as in the developing forebrain (Fig. 2A). At E11.5, *Foxg1* expression was absent from the distal rim of the OP, and became restricted to the central region, where neuronal differentiation is taking place (Fig. 2B) (Kawauchi et al., 2005). As development proceeds (E12.5 to E17.5), *Foxg1* expression is maintained in the OE, but becomes progressively restricted to the basal compartment of the epithelium, where stem and neuronal progenitor cells are located (Fig. 2C-E) (Beites et al., 2005).

Gdf11 expression is first evident at E10.5 in the epithelium of the OP, and is also observed outside of the OE proper, in what are probably the migrating olfactory pioneer neurons that demarcate the pathway of the developing olfactory nerve (Fig. 2A) (Astic et al., 2002). By E12.5, *Gdf11* expression expands to include the entire sensory neuroepithelium of the OE, and this pattern is maintained throughout development (Fig. 2C-E) (Nakashima et al., 1999; Wu et al., 2003).

Overall, the expression domain of *Gdf11* overlaps substantially with that of *Foxg1* throughout pre-natal development. As *Gdf11* is known to both be expressed by, and act upon, OE neuronal progenitor cells (Lander et al., 2009; Wu et al., 2003), *Foxg1*-expressing cells are in the correct locations and at the right times to be targets of Gdf11.

Interestingly, the expression of *Foxg1* throughout the lateral extent of the OE is not uniform. By E12.5, there are clear regional differences: *Foxg1* expression is highest at locations such as the recesses of the developing turbinates and the posterior recess of the nasal cavity (at the junction of the septum and the turbinates). By comparing such patterns over time, it can be seen that the locations of high *Foxg1* expression represent the sites where the OE is most actively expanding into the nasal mesenchyme. By contrast, *Gdf11* expression is rather uniformly expressed wherever OE is present (Fig. 2C-E, and insets).

p21Cip1 expression is regulated by *Gdf11* and *Foxg1* in early OE development

Fox gene products affect cell proliferation and cell cycle dynamics in several cell types, including neural cells (Dou et al., 2000; Gomis et al., 2006; Hanashima et al., 2002; Martynoga et al., 2005), and it has been proposed that the major role of Foxg1 in cortical development is to promote neural precursor proliferation (Xuan et al., 1995). To quantify stem/progenitor cell proliferation in the OE of *Foxg1*$^{-/-}$ mice, we performed pulse-fix experiments at E11 and E12, using BrdU to label cells in S-phase (Fig. 3A). At both ages, the number of BrdU-immunopositive cells in any given section through the OE was much lower in *Foxg1*$^{-/-}$ mice, as was the overall size of the OE. Even if the discrepancy in size was corrected for by normalizing the number of BrdU-immunopositive cells to the linear distance along the basal lamina of the epithelium, 44% less labeling was still observed in *Foxg1*$^{-/-}$ OE than in wild type (at E11.0: wild type, 207±4 BrdU^{+} cells/mm OE; *Foxg1*$^{-/-}$, 121±6 BrdU^{+} cells/mm OE).

Interestingly, this change in BrdU labeling in *Foxg1*$^{-/-}$ OE was accompanied by an expansion of expression of the CKI *p21Cip1* (Fig. 3B). At E10.5, expression of *p21Cip1*, which at later stages of OE development correlates with neuronal differentiation (Kastner et al., 2000; Legrier et al., 2001), was normally confined to the rim of the invaginating nasal pit (Fig. 3B). In *Foxg1*$^{-/-}$ OE, however, *p21Cip1* expression was expanded to include both the rim and the central region of the OE. This finding suggests that increased *p21Cip1* expression in *Foxg1*$^{-/-}$ OE might contribute to the alterations in the number of cycling cells and the deficits in neuronal cell differentiation observed in these mutants.

In cultured neural cells and cell lines, it has been shown that Foxg1 can repress *p21Cip1* induction effected by TGFβ signaling (Dou et al., 2000; Rodriguez et al., 2001; Seoane et al., 2004). Because Gdf11 acts through the same intracellular effectors as TGFβ, we investigated whether Gdf11 controls the expression of *p21Cip1* in the OE. Two types of experiments were done. First, we performed ISH for *p21Cip1* in *Gdf11* nulls and their wild-type littermates. As shown in Fig. 3C, *p21Cip1* levels were greatly reduced in the OE of E13.5 *Gdf11*$^{-/-}$ animals, implying that *Gdf11* is a positive regulator of *p21Cip1* expression in vivo. Second, we cultured OE explants from wild-type embryos at a similar age (E15.5), and examined expression of p21Cip1 by immunofluorescence after 14 hours' growth in the presence or absence of recombinant Gdf11. The results are shown in Fig. 3D. As described previously, neuronal cells (neuronal progenitors and immature ORNs) comprise virtually all of the migratory cells in explant cultures of OE purified from mouse embryos at this age (Calof and Chikaraishi, 1989; DeHamer et al., 1994; Mumm et al., 1996). Figure 3D shows that only a small percentage (2.5%) of neuronal cells in untreated control cultures showed significant p21Cip1 immunoreactivity. By contrast, the percentage of p21Cip1-immunoreactive neuronal cells was more than fivefold greater in GDF11-treated cultures (14.3%). Thus, GDF11 treatment causes an increase in p21Cip1 expression in OE neuronal progenitors and/or immature ORNs.

Inactivation of *Gdf11* rescues neurogenesis in *Foxg1*$^{-/-}$ OE

The presence of *Gdf11* and *Foxg1* at similar times and locations in the OE, the known ability of Foxg1 to inhibit the induction of TGFβ pathway target genes that are also induced by Gdf11, and the oppositely directed effects of *Gdf11* and *Foxg1* mutations on OE neurogenesis, all raise the possibility that Foxg1 acts via inhibition of Gdf11 activity. To assess this directly, we compared OE development in wild type, *Foxg1*$^{-/-}$, *Gdf11*$^{-/-}$ and *Foxg1*$^{-/-}$;*Gdf11*$^{-/-}$ double mutants. Morphology and neuronal lineage markers were first examined at birth (the latest age to which both strains survive) in sagittal sections at equivalent mediolateral levels (Fig. 4A). Figure 4B-D shows ISH analysis of littermate wild-type, *Foxg1*$^{-/-}$ and *Foxg1*$^{-/-}$;*Gdf11*$^{-/-}$ animals, performed using a probe to *Ngn1* to highlight the neuronal progenitor layer of the OE (Beites et al., 2005; Wu et al., 2003). As shown in Fig. 4B, the nasal cavity and turbinate cartilage underlying the nasal mucosa are easily visualized in sections from wild-type mice, with *Ngn1*+ progenitor cells forming a distinct layer in the basal region of the OE proper. In sections from *Foxg1*$^{-/-}$ mice, however, no olfactory turbinate structures were observed: Only a small cavity filled with serous gland tubules was seen, and no expression of *Ngn1* could be detected (Fig. 4C). By

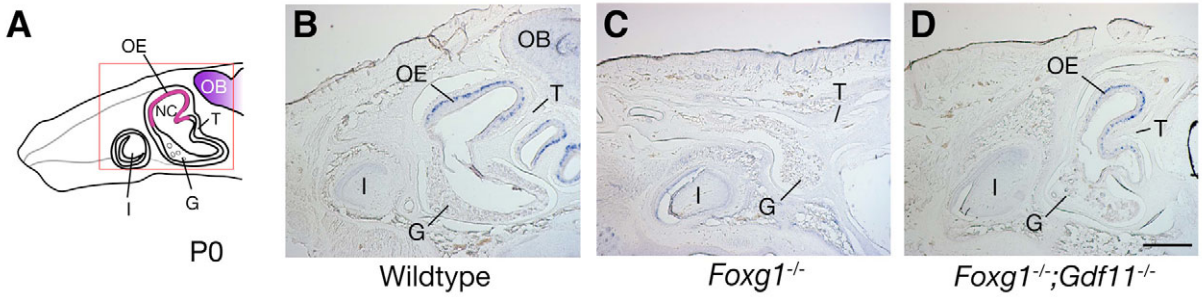

Fig. 4. Rescue of the *Foxg1*$^{-/-}$ OE phenotype by loss of *Gdf11*. (**A**) Cartoon of normal frontonasal structures in mice at P0, shown as a mid-sagittal section. Red square indicates the region photographed for ISH images shown in B-D. G, serous gland; I, right upper incisor; OB, olfactory bulb; OE, olfactory epithelium; T, turbinate bone; NC, nasal cavity. (**B**) ISH for *Ngn1* to show OE neuronal cells in wild-type animals at P0. (**C**) Olfactory turbinate structures and *Ngn1*-expressing OE are not observed in *Foxg1*$^{-/-}$ animals. (**D**) *Foxg1*$^{-/-}$;*Gdf11*$^{-/-}$ mice show recovery of turbinate structures and OE expressing *Ngn1*. Note that there is no OB present in either *Foxg1*$^{-/-}$ or *Foxg1*$^{-/-}$;*Gdf11*$^{-/-}$; note also that the telencephalon is drastically reduced in *Foxg1*$^{-/-}$ mice and is not rescued by loss of *Gdf11* (see Results). Scale bar: 500 μm.

contrast, both the gross morphology of nasal structures and the microscopic structure of the OE are significantly rescued in *Foxg1;Gdf11* double mutants (Fig. 4D). The double mutants have recognizable olfactory turbinates that are lined with OE, and this OE contains *Ngn1*$^{+}$ cells in their normal, basal, location. This OE surrounds a substantial nasal cavity that is located dorsal and posterior to the major maxillary incisor, as is the case in wild-type animals (compare Fig. 4B and 4D). Thus, the absence of *Gdf11* results in substantial rescue of the defects in nasal cavity morphogenesis and OE neuroepithelial development observed in *Foxg1*$^{-/-}$ mice.

To determine when such rescue occurs, we examined OE neuronal lineage markers in horizontal sections of heads from E13.5 embryos that were null for *Gdf11*, *Foxg1*, or both genes, and compared these with sections from wild-type littermates. The results are shown in Fig. 5. In wild-type mice at E13.5, cells expressing all four major stage-specific markers (*Sox2*, *Mash1*, *Ngn1* and *Ncam*) were present in the OE (Fig. 5A). In *Gdf11*$^{-/-}$ mice at this age, the OE was essentially identical to wild type; increases in neuronal cells above wild-type numbers was not evident until a later stage of development in these mutants (Fig. 5B) (cf. Wu et al., 2003). In contrast to wild-type and *Gdf11*$^{-/-}$ embryos, *Foxg1*$^{-/-}$ embryos at E13.5 have essentially no OE (Fig. 5C). When viewed at a dorsoventral level equivalent to the wild-type example (note presence of retina in all sections), the *Foxg1*$^{-/-}$ embryo shown in Fig. 5C shows reduction of the entire frontonasal region, an absence of nasal cavities, and an aberrant (apparently enlarged) optic recess of the third ventricle. When *Foxg1*$^{-/-}$ embryos were also made null for *Gdf11*, however, both the OE and the frontonasal region were significantly rescued at E13.5 (Fig. 5D). The OE of *Foxg1*$^{-/-}$*;Gdf11*$^{-/-}$ embryos was of normal thickness, and contained cells expressing all major neuronal lineage markers (Fig. 5D). Moreover, a developing nasal cavity could be seen, as well as lateral folds of mesenchyme covered by OE, evidence that basic turbinate structures are also rescued in the double mutant (Fig. 5D). Thus, the failure of both OE neurogenesis and nasal cavity morphogenesis observed in *Foxg1*$^{-/-}$ animals is significantly rescued by E13.5 when *Gdf11* is absent.

Gdf11 dosage regulates the ability of *Foxg1* to maintain OE neurogenesis

Genes of the TGFβ superfamily often show dose dependence in their effects on development (Dunn et al., 1997; Eldar et al., 2002; Lawson et al., 1999; Sutherland et al., 2003). We tested whether *Gdf11* might show such activity in its effects on OE development. Mice null for *Gdf11*, *Foxg1*, as well as *Foxg1*$^{-/-}$*;Gdf11*$^{+/-}$ and *Foxg1*$^{-/-}$*;Gdf11*$^{-/-}$ mice, were examined at E16.5 (Fig. 6). At this stage in normal development, olfactory turbinates are well developed and all cell types in the OE can be recognized easily by their laminar position and molecular marker expression; at this stage, the OE also possesses an apical layer of sustentacular cells, the intrinsic glial cells of the OE (Beites et al., 2005; Cuschieri and Bannister, 1975a; Cuschieri and Bannister, 1975b; Murray et al., 2003; Smart, 1971). As demonstrated previously (Wu et al., 2003), *Gdf11* nulls at this age have greater numbers of *Ngn1*-expressing INPs and *Ncam*-expressing ORNs than wild types, but show no obvious changes in the number of *Mash1*-expressing early neuronal progenitors (Fig. 6A,B). We have found that *Otx2*, an orthodenticle homolog that is expressed in the developing olfactory placode (Mallamaci et al., 1996), is a marker for sustentacular cells at E16.5 and beyond in the mouse OE. Figure 6B shows that the layer of *Otx2*-expressing sustentacular cells appears to be complete in *Gdf11* mutants, as expected.

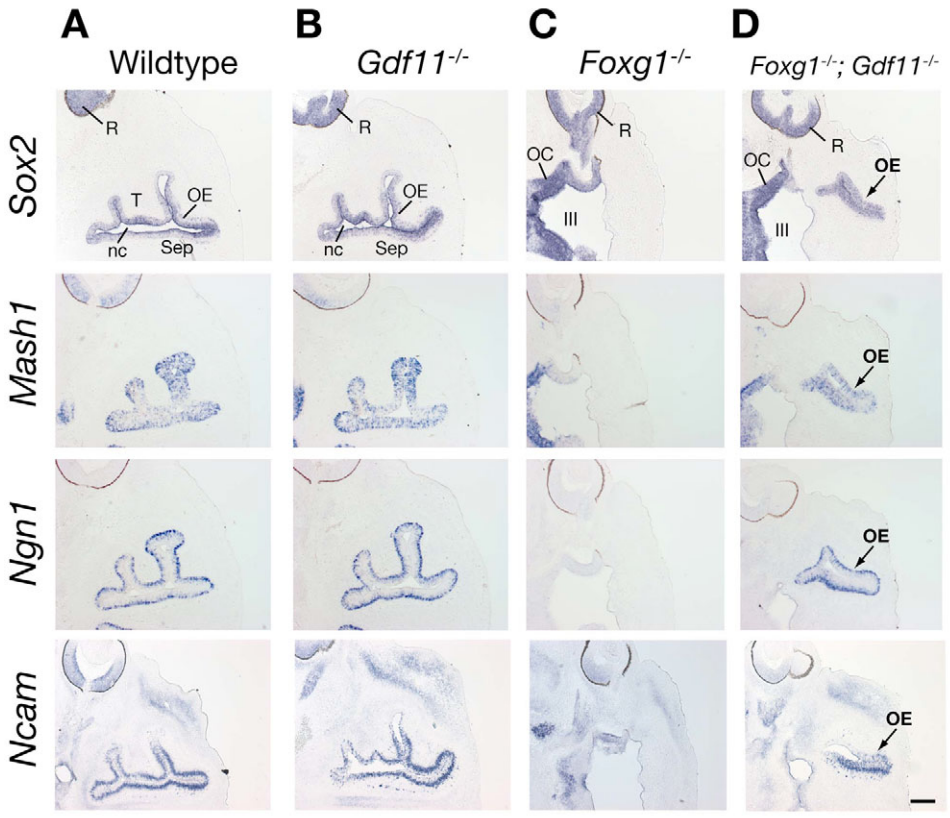

Fig. 5. Significant rescue of the *Foxg1*$^{-/-}$ OE phenotype occurs by E13.5. Horizontal sections through heads of E13.5 wild-type and *Gdf11*$^{-/-}$ embryos, hybridized with probes for indicated OE neuronal lineage markers. (**A**,**B**) Identical patterns of expression are observed in wild-type and *Gdf11*$^{-/-}$ OE at this age. OE, olfactory epithelium; nc, nasal cavity; R, retina; Sep, septum; T, turbinate. (**C**) *Foxg1*$^{-/-}$ embryos lack OE, a nasal cavity, and all OE neuronal lineage markers by E13.5. III, ventral portion of third ventricle; OC, optic chiasm. (**D**) Substantial rescue of the OE and nasal cavity structures, as well as cells expressing all OE neuronal lineage markers, is observed in *Foxg1*$^{-/-}$*;Gdf11*$^{-/-}$ embryos. Scale bar: 200 μm.

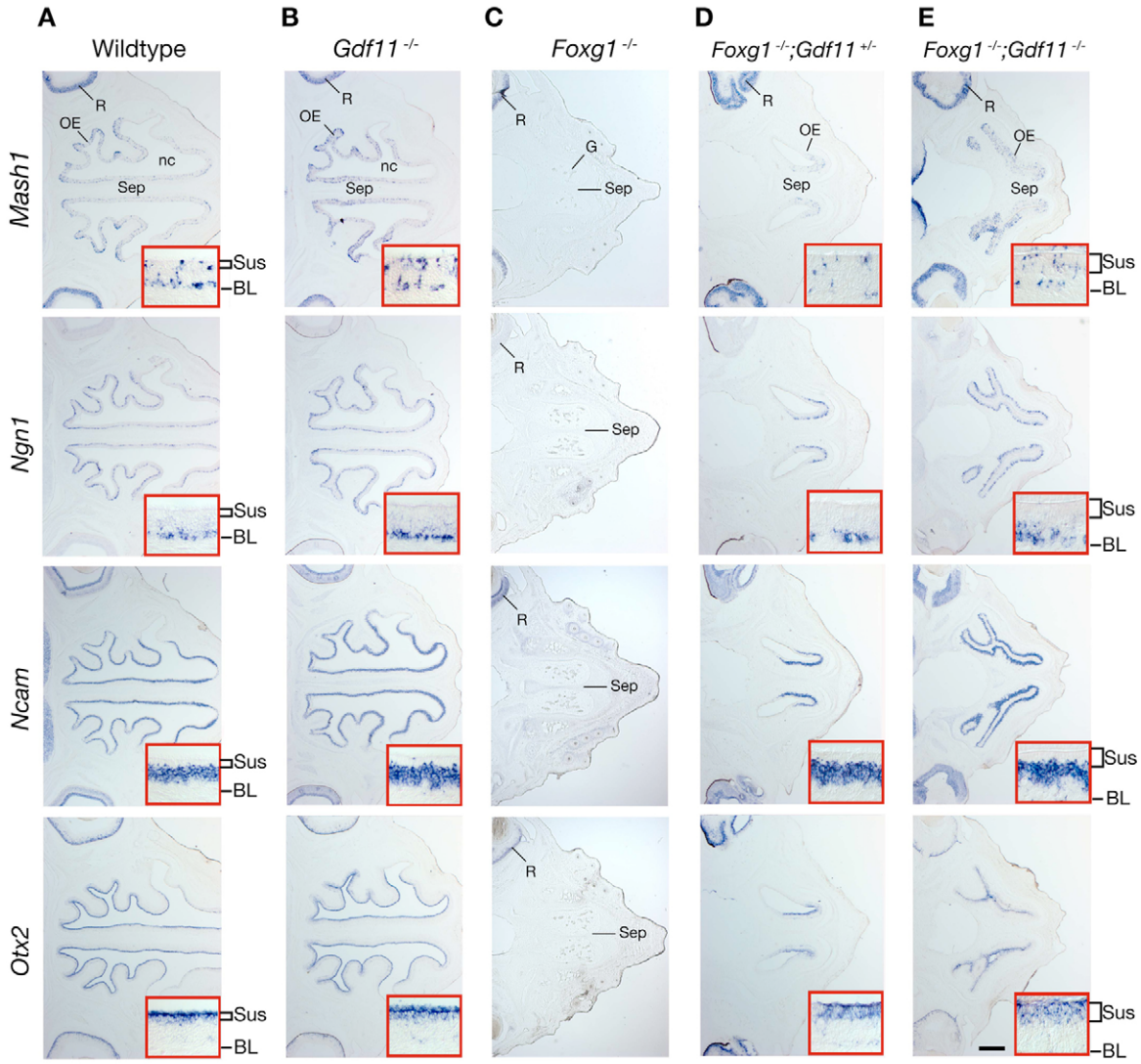

Fig. 6. Rescue of OE neurogenesis in *Foxg1*$^{-/-}$ mutants is dependent on *Gdf11* gene dosage. ISH for OE neuronal lineage markers (*Mash1*, *Ngn1* and *Ncam*) and sustentacular cells (*Otx2*), performed on horizontal sections through the OE of E16.5 wild-type and mutant littermates. Insets show high magnification views of septal OE. (**A**,**B**) OE and cell types within it are similar in wild-type and *Gdf11*$^{-/-}$ mice at this age, except that *Ngn1*- and *Ncam*-expressing cell layers (and hence OE overall) are thicker, as reported previously (Wu et al., 2003). (**C**) No OE structure (apart from a truncated septum), nor any cell type-specific markers, are evident in sections from *Foxg1*$^{-/-}$ mice at the same dorsoventral level. (**D**) Loss of one *Gdf11* allele (*Foxg1*$^{-/-}$;*Gdf11*$^{+/-}$) rescues all cell types in the OE, and the OE appears to be of normal thickness, although planar expanse of the OE and morphogenesis of nasal cavity are clearly deficient in the compound mutant. (**E**) Rescue is more pronounced in *Foxg1*$^{-/-}$;*Gdf11*$^{-/-}$ double mutants, particularly in terms of OE planar expanse and nasal cavity morphogenesis. For all panels, posterior is left, anterior is right. Sus, sustentacular cells; BL, basal lamina. Scale bar: 400 μm.

In contrast to what was seen in wild-type and *Gdf11*$^{-/-}$ embryos at E16.5, the OE neuroepithelium itself, the nasal cavity, and molecular markers of OE neuronal and sustentacular cells were largely absent from *Foxg1*$^{-/-}$ embryos at this age, despite the fact that a septal structure could often be observed (Fig. 6C) (the presence of neural retina in all sections indicates that the horizontal sections shown have been taken at approximately the same dorsoventral level). Notably, when just one allele of *Gdf11* was inactivated in *Foxg1* nulls (*Foxg1*$^{-/-}$;*Gdf11*$^{+/-}$ embryos), bilateral nasal cavities formed and were easily recognizable in the compound mutants at E16.5 (Fig. 6D). Although the surfaces of the nasal cavities were not as elaborately folded as in wild-type OE, they were lined by an OE of normal thickness. Moreover, the OE in these compound mutants contained cells expressing all neuronal and sustentacular markers tested, and these cells were present in their appropriate apical-basal positions within the OE (compare Fig. 6D to 6A). Indeed, even the layer of *Ncam*-expressing ORNs appeared to be as thick as that seen in wild types (Fig. 6D, inset).

When two alleles of *Gdf11* were inactivated, the rescue of nasal cavity morphogenesis and OE neurogenesis was even more pronounced. As shown in Fig. 6E, cells expressing neuronal and sustentacular markers were found in their appropriate layers, and turbinates had developed as folds of differentiating mesenchyme that protrude into the nasal cavities; these were substantially larger and more elaborate in shape than those seen in compound mutants in which only one allele of *Gdf11* was inactivated. Interestingly, the

pattern of *Otx2* expression in the layer of sustentacular cells of *Foxg1*$^{-/-}$;*Gdf11*$^{-/-}$ OE was noticeably diffuse when compared with that observed in wild-type and *Gdf11*$^{-/-}$ OE (compare Fig. 6E with 6A,B). This observation suggests that *Foxg1* may be involved in sustentacular cell differentiation.

Altogether, the observations described above support the conclusion that *Foxg1* exerts its effects on OE neurogenesis through quantitative antagonism of *Gdf11* activity. In view of the known interaction of Foxg1 with Smad transcriptional complexes, it is reasonable to propose that the effects of Foxg1 are mediated through a direct, cell-autonomous influence on signaling downstream of Gdf11. However, as described below, additional effects may come into play as well.

Loss of follistatin expression in *Foxg1*$^{-/-}$ nasal mucosa and its rescue by loss of *Gdf11*

The secreted protein follistatin (Fst) is an antagonist of activins and Gdf11 that competes for binding of these factors to their receptors (Gamer et al., 2001; Nakamura et al., 1990; Schneyer et al., 1994; Schneyer et al., 2008; Wu et al., 2003). Fst is expressed in the nasal mucosa, both in the OE proper and in its underlying mesenchymal stroma (Lander et al., 2009; Wu et al., 2003); during embryonic development, stromal expression of *Fst* is particularly strong (Fig. 7A). The importance of Fst as an endogenous inhibitor of GDF11 is evidenced by the phenotype of *Fst*$^{-/-}$ mice, which display an OE at birth that is very thin and that is markedly depleted of neurons (Wu et al., 2003).

Intriguingly, we found that *Foxg1*$^{-/-}$ embryos lack *Fst* expression in and around the OE from the earliest developmental stages (Fig. 7A). Even when OE remnants could be detected at late stages in *Foxg1*$^{-/-}$ embryos (e.g. example in Fig. 7A at E16.5), no *Fst* expression was detected. These results suggest an additional mechanism by which *Foxg1* could antagonize *Gdf11* activity: by promoting expression of Fst, a Gdf11 antagonist, *Foxg1* could lower the effective concentration of Gdf11 in the extracellular milieu. Although this latter activity might contribute to the *Foxg1*$^{-/-}$ phenotype in the OE, however, it cannot explain it entirely, as that phenotype is both qualitatively and quantitatively different from the OE phenotype observed in *Fst*$^{-/-}$ mice (see Fig. S1 in the supplementary material; see also Discussion). It seems more likely that the *Foxg1*$^{-/-}$ phenotype arises as the result of a combination of intracellular (cell-autonomous) and extracellular (non-cell-autonomous) effects. This may help to explain why the phenotype is so severe.

Interestingly, both stromal and intraepithelial expression of *Fst* were completely rescued not only in *Foxg1*$^{-/-}$;*Gdf11*$^{-/-}$ embryos, but also in compound *Foxg1*$^{-/-}$;*Gdf11*$^{+/-}$ mutants in which only one allele of *Gdf11* was inactivated (Fig. 7B). This demonstrates that *Foxg1* is not itself required for *Fst* expression, i.e. Foxg1 does not itself induce *Fst*. The most parsimonious explanation is that it is the OE itself that induces *Fst* in surrounding tissue, with Foxg1 being required to generate an OE that is competent to do so. Exactly what signal from the OE induces *Fst* is unknown, but from the data in Fig. 7B, we can rule out Gdf11.

Does *Foxg1* regulate *Gdf11* expression?

In view of the fact that Foxg1 is a transcriptional regulator, we also considered the possibility that a third mechanism – a repressive effect of Foxg1 on *Gdf11* expression – might also be at play in the OE. To investigate this, we measured the expression of *Gdf11* in the different mutants discussed above. The results of these experiments, shown in Fig. 8, revealed several interesting findings. First, we found no evidence that *Gdf11* autoregulates its own expression, as is the case for some TGFβ superfamily members (Fig. 8A) (Chen and Schier, 2002; Forbes et al., 2006). Thus, in a normal (wild-type) genetic background, inactivation of one allele of *Gdf11* led to a reduction in *Gdf11* transcript levels to 35-49% of wild type; loss of both alleles led to essentially undetectable expression of *Gdf11* (Fig. 8A). Second, in the frontonasal process of E12 *Foxg1*$^{-/-}$ embryos, where loss of OE tissue was already significant, *Gdf11* expression was still detectable in the remaining OE by ISH (Fig. 8B).

Third, Q-RT-PCR experiments, performed to determine transcript levels of *Gdf11* in E11.5 frontonasal tissue (this age was chosen because there is still a reasonable amount of OE remaining in *Foxg1*-null animals), showed that *Gdf11* transcript levels in *Foxg1*$^{-/-}$ and *Foxg1*$^{-/-}$;*Gdf11*$^{+/-}$ mutants were significantly lower than in wild type (Fig. 8C). This was not surprising, given that *Gdf11* is mainly expressed in the OE, and there is substantially less OE tissue in such mutants compared with wild type. Indeed, Q-RT-PCR showed that levels of *Sox2*, a marker for neuroepithelium (Fig. 1A), were also markedly decreased in *Foxg1*$^{-/-}$ and *Foxg1*$^{-/-}$;*Gdf11*$^{+/-}$ mutants (Fig. 8D). By normalizing *Gdf11* transcript levels to *Sox2* transcript levels

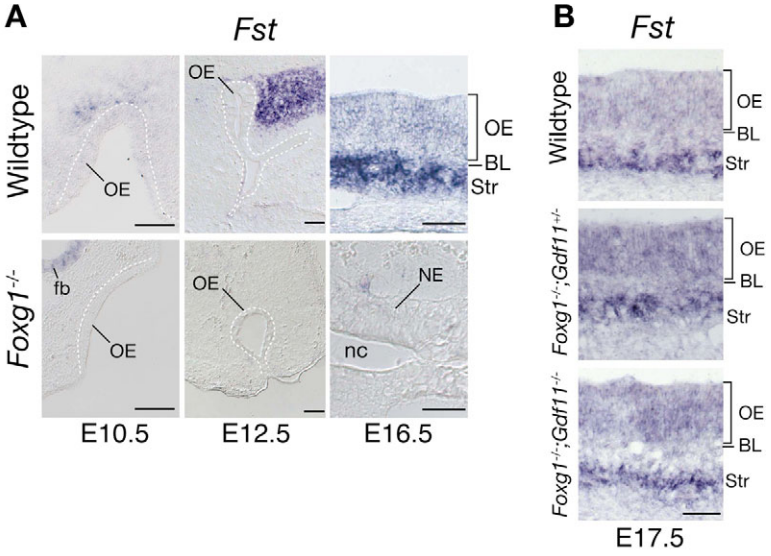

Fig. 7. Downregulation of *Fst* expression in *Foxg1*$^{-/-}$ nasal mucosa is rescued by loss of *Gdf11*. (**A**) ISH for *Fst* performed on coronal sections through heads of wild-type and *Foxg1*$^{-/-}$ mice at E10.5 and E12.5, and on horizontal sections at E16.5. At E16.5, when *Fst* is expressed in both the OE and stroma of nasal mucosa in wild types (A, top right panel), *Fst* expression is undetectable in *Foxg1*$^{-/-}$ embryos in rare instances when remnants of nasal mucosa are observed (A, bottom right panel). NE, nasal epithelium; OE, olfactory epithelium; BL, basal lamina; nc, nasal cavity; Str, stroma; fb, forebrain. Scale bars: 100 μm in E10.5 and E12.5; 50 μm in E16.5. (**B**) *Fst* expression is restored in the OE and underlying stroma of *Foxg1*$^{-/-}$;*Gdf11*$^{+/-}$ and *Foxg1*$^{-/-}$;*Gdf11*$^{-/-}$. Scale bar: 50 μm.

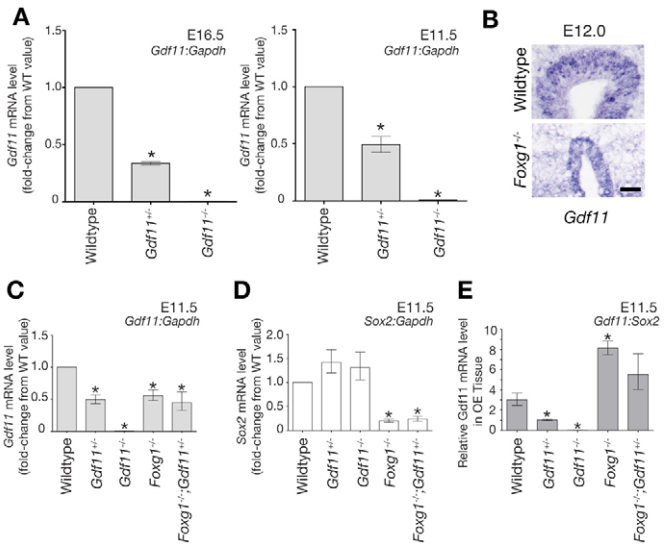

Fig. 8. Analysis of *Gdf11* mRNA expression in the OE of embryos of different genotypes. (**A**) *Gdf11* does not regulate its own transcription. *Gdf11* and *Gapdh* transcript levels at E16.5 and E11.5 were quantified by Q-RT-PCR, and dCT and ddCT values with errors were calculated as described in the Materials and methods. For presentation purposes, data are normalized to wild-type values. Statistics [Dunnett's test for multiple comparisons against a single control (DT) (Glantz, 2005)] were performed using mean dCT values and corresponding errors (s.e.m.), which were: E16.5, wild type=5.32±0.0233; $Gdf11^{+/-}$=6.89±0.0523, $Gdf11^{-/-}$=13.53±0.4933; E11.5, wild type=5.22±0.200, $Gdf11^{+/-}$=6.24±0.009, $Gdf11^{-/-}$=12.22±0.142. (**B**) *Gdf11* is expressed in $Foxg1^{-/-}$ OE at E12.0. ISH for *Gdf11* was performed on coronal cryosections of wild type and $Foxg1^{-/-}$. Scale bar: 50 μm. (**C-E**) Relative *Gdf11* and *Sox2* expression values in OE from E11.5 embryos of different genotypes. *Gdf11*, *Sox2,* and *Gapdh* transcript levels were quantified by Q-RT-PCR as described in the Materials and methods. In C and D, *Gdf11:Gapdh* and *Sox2:Gapdh* expression levels are normalized to wild-type values for presentation purposes. Statistics (DT) were performed using mean dCT values and corresponding errors (s.e.m.), which were as follows: *Gdf11*:*Gapdh*, wild type=5.22±0.200, *n*=3; $Gdf11^{+/-}$=6.24±0.009, *n*=2; $Gdf11^{-/-}$=12.22±0.142, *n*=3; $Foxg1^{-/-}$=6.07±0.088, *n*=3; $Foxg1^{-/-};Gdf11^{+/-}$=6.39±0.422, *n*=3. *Sox2*:*Gapdh*: wild type=6.81±0.217, *n*=3; $Gdf11^{+/-}$=6.30±0.116, *n*=3; $Gdf11^{-/-}$=6.42±0.230, *n*=3; $Foxg1^{-/-}$=9.09±0.083, *n*=3; $Foxg1^{-/-};Gdf11^{+/-}$=8.85±0.176, *n*=3. (E) *Gdf11* expression plotted as the ratio of the mean *Gdf11* transcript level to the mean *Sox2* level. Values that differ significantly from wild type ($P<0.05$, DT) are denoted by asterisks.

in the same samples, we could attempt to correct for the differing amounts of OE in different samples. The results (Fig. 8E) indicated that *Gdf11* levels were 2- to 3-fold higher, per unit of OE, in *Foxg1* nulls than in wild-type animals.

Defects in cerebral cortex development in $Foxg1^{-/-}$ embryos are not rescued by loss of *Gdf11*

Because *Gdf11* is expressed in some regions of the telencephalon (Nakashima et al., 1999), we considered the possibility that absence of *Gdf11* might also rescue some of the defects in telencephalic neurogenesis that are observed in *Foxg1* mutants (Hanashima et al., 2007; Hanashima et al., 2004; Hanashima et al., 2002; Hebert and McConnell, 2000; Xuan et al., 1995). When we examined $Foxg1^{-/-};Gdf11^{-/-}$ embryos, however, we found no such rescue. This is illustrated in Fig. 9A, which shows Hematoxylin/Eosin-stained horizontal sections through the brains of E13.5 mice of the three different genotypes. As noted previously (Xuan et al., 1995), the developing cerebral hemispheres were much smaller in $Foxg1^{-/-}$ embryos than in wild types and, instead of a smooth cortical neuroepithelium, the cortical surface was buckled and uneven, and cortical thickness differed in different areas. In $Foxg1^{-/-};Gdf11^{-/-}$ double mutants, there was no rescue of this phenotype: the cerebral hemispheres were still much smaller than in wild-type embryos, and the cortex showed the same structural aberrations that are apparent in $Foxg1^{-/-}$ embryos. Thus, absence of *Gdf11* fails to rescue the defects in cortical development seen in the *Foxg1*-null mouse.

To understand why an absence of *Gdf11* should fail to rescue cortical development, while OE development is rescued so dramatically, we performed ISH to examine the expression of *Gdf11* and *Foxg1* in the developing forebrain from E11.5 through E15.5. As shown in Fig. 9B, *Foxg1* was initially expressed throughout the telencephalon, but gradually became restricted to more dorsal structures, including the developing cerebral cortex. By contrast, *Gdf11* expression at E11.5 was primarily found in a subset of the most ventral cells, but gradually disappeared by E15.5. Thus, cells that express *Gdf11* appear not to be located in the vicinity of the developing cortical neuroepithelium.

DISCUSSION

Foxg1 activity supports a self-sustaining neurogenic network

The experiments described above demonstrate that *Foxg1* promotes OE neurogenesis in large part through the antagonism of *Gdf11*. Of the possible mechanisms by which this effect may be achieved, the simplest, and most direct, involves the known interaction of Foxg1 with Smad signaling complexes to inhibit Smad-dependent transcription (Dou et al., 2000; Massague and Gomis, 2006; Rodriguez et al., 2001; Seoane et al., 2004). Although that interaction was discovered through the study of *p21Cip1* induction by TGFβ1 in cultured cells and cell lines, Gdf11 acts through the same Smads as TGFβ1 (Nomura et al., 2008; Tsuchida et al., 2007), and, we have shown that Gdf11 induces *p21Cip1* in cells of the OE (Fig. 3). Recent studies in the zebrafish, in which morpholino oligonucleotides were used to reduce Foxg1 levels in a mosaic fashion (Duggan et al., 2008), also showed that Foxg1 influences OE neurogenesis in a cell-autonomous fashion, a result opposite to what would have been expected if Foxg1 acts by controlling the expression of a secreted growth factor, such as an FGF.

The fact that we observe a higher level of *Gdf11* transcripts, relative to *Sox2* transcripts, in *Foxg1* mutant OE (Fig. 8E) raises the additional possibility that Foxg1 regulates the expression of *Gdf11* at the transcriptional level, although we cannot rule out alternative interpretations of the data. For example, loss of Foxg1 in $Foxg1^{-/-}$ OE might increase the number of *Gdf11*-expressing cells (relative to *Sox2*-expressing cells), rather than the level of *Gdf11* transcripts per cell. Conversely, loss of Foxg1 might decrease the expression of *Sox2*. Even if Foxg1 does regulate *Gdf11* transcription, the mechanism need not be direct (i.e. it could be mediated through other Foxg1 target genes). Likewise, loss of expression of the extracellular Gdf11 antagonist Fst in and around the OE of $Foxg1^{-/-}$ mice almost certainly reflects an indirect effect, as *Foxg1* is not expressed in the stroma (where most *Fst* expression occurs), and *Fst* expression can be achieved in the complete absence of *Foxg1* OE, by removing copies of *Gdf11*.

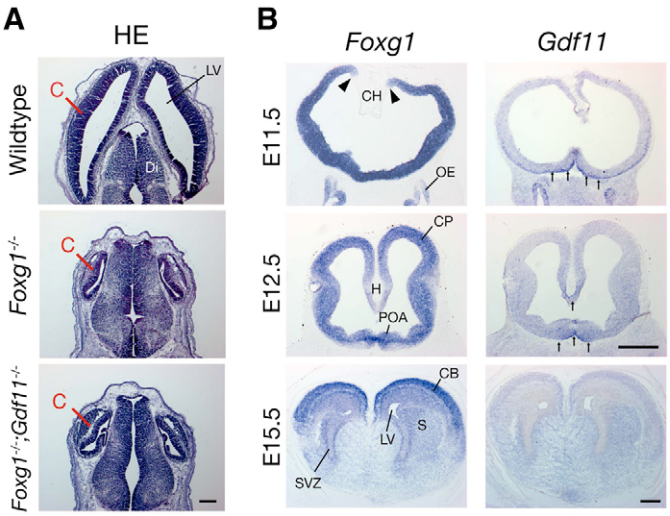

Fig. 9. Absence of *Gdf11* does not rescue defects in *Foxg1*$^{-/-}$ cerebral cortex. (**A**) Hematoxylin and Eosin staining of horizontal sections through the brains of wild type, *Foxg1*$^{-/-}$, and *Foxg1*$^{-/-}$;*Gdf11*$^{-/-}$ double mutants at E13.5. The cortex is severely reduced in *Foxg1*$^{-/-}$ embryos; absence of *Gdf11* does not rescue this phenotype. Scale bar: 200 μm. (**B**) Expression of *Foxg1* and *Gdf11* in coronal sections through developing mouse brain. *Foxg1* is abundantly expressed in the telencephalon (except for the cortical hem) at E11.5 (expression boundary indicated by arrowheads). *Gdf11* expression is apparent in the ventral telencephalon and OE at E11.5, but by E12.5 is restricted to ventral midline of the telencephalon and the nascent hippocampus (arrows). At E15.5, no *Gdf11* expression is apparent in the rostral telencephalon, whereas *Foxg1* levels are high, especially in dorsal areas. Scale bars: 400 μm. C, cortex; CB, cerebral cortex; CH, cortical hem; CP, cortical plate; Di, diencephalon; H, hippocampus; LV, lateral ventricle; OE, olfactory epithelium; S, striatum; POA, preoptic area; SVZ, subventricular zone.

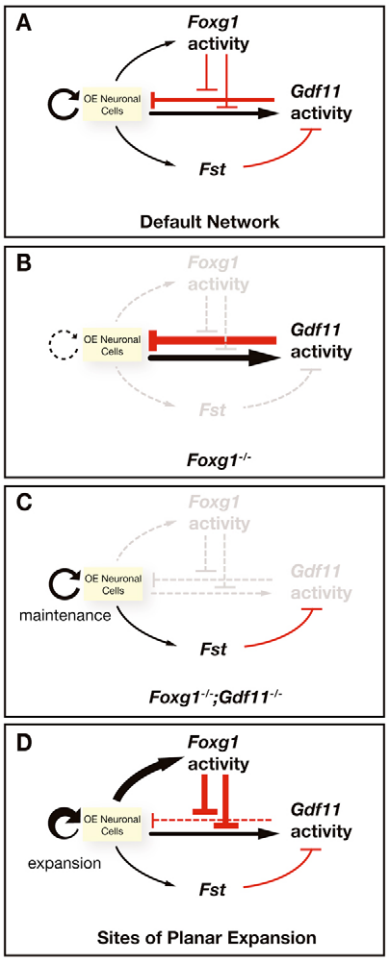

Fig. 10. Schematic model of *Foxg1-Gdf11* interactions controlling OE neurogenesis. (**A**) In wild-type OE, *Foxg1* and *Gdf11* are both produced by OE neuronal cells, but *Foxg1* pro-neurogenic activity antagonizes both the anti-neurogenic activity of *Gdf11* and the production of *Gdf11* by OE neuronal cells. *Fst* is also expressed by OE neuronal cells, and *Fst* action antagonizes *Gdf11* activity. This default network of gene activities controls the normal steady-state level of neurogenesis in the OE. (**B**) In *Foxg1*$^{-/-}$ OE, *Foxg1* activity is absent, *Fst* expression is downregulated, and *Gdf11* expression is upregulated, resulting in hypersensitivity of the frontonasal region and OE to the action of *Gdf11*. Both OE neurogenesis and planar expansion of the OE fail. (**C**) In the *Foxg1*$^{-/-}$;*Gdf11*$^{-/-}$ double mutant, *Fst* expression is restored and histogenesis (neurogenesis) within the OE is rescued, as the anti-neurogenic activity of *Gdf11* is now removed and any similar anti-neurogenic factors are antagonized by *Fst*. (**D**) *Foxg1* activity strongly inhibits both *Gdf11* activity and expression, which would allow the OE to undergo planar expansion in sites where *Foxg1* is highly expressed in wild-type OE (e.g. posterior recess of the nasal cavity). Once expansive growth is finished, *Foxg1* expression is downregulated (e.g. in the anterior septum), and OE neurogenesis returns to its default state.

Regardless of the underlying mechanism(s), however, the finding that loss of *Foxg1* is capable of leading to increased Gdf11 signaling, increased *Gdf11* expression, and decreased expression of a Gdf11 antagonist collectively suggest that the relationship between Gdf11 activity and Foxg1 activity is a highly sensitive one.

At the same time, a highly sensitive relationship also appears to exist between *Gdf11* activity and the capacity of OE cells for neurogenesis. The fact that removal of a single *Gdf11* allele transforms a *Foxg1*$^{-/-}$ embryo from one in which no OE or nasal cavity develops, into one with an OE of normal thickness and composition, suggests that there is a threshold level of Gdf11 activity below which neurogenesis proceeds fairly normally, and above which neurogenesis fails completely.

Threshold responses to signaling molecules usually imply cooperativity (or some other form of ultrasensitivity), such that a doubling in gene dosage produces more than a doubling in signaling. Because *Gdf11* does not appear to regulate its own expression (Fig. 8A), we believe the likely source of ultrasensitivity lies elsewhere. If, as we suggest, the OE induces expression of *Fst* in its underlying stroma, then a positive-feedback loop emerges: an increase in *Gdf11* activity would lead to a decrease in OE size, which would cause a decrease in *Fst* expression, which would in turn cause an increase in *Gdf11* activity. A decrease in *Gdf11* activity would be similarly self-enhancing. According to this view, Gdf11 in the embryonic OE is less of a graded regulator of neuronal production than a switch-like controller of a self-sustaining program of neurogenesis, with Foxg1 regulating when and where the switch is thrown.

Foxg1 and olfactory epithelium morphogenesis

During embryonic development of the OE, the process of neurogenesis can be viewed as serving two distinct ends: histogenesis and morphogenesis. By histogenesis we mean the

generation of an appropriate complement and number of OE cells at each location along the epithelium. By morphogenesis we mean the planar growth and invagination of the epithelium to produce a deep, characteristically folded nasal cavity. In *Foxg1*$^{-/-}$ embryos, both processes fail from early stages. Yet when *Foxg1* mutants are rescued through loss of *Gdf11*, the two processes are restored to very different degrees. Histogenesis is nearly normal in both *Foxg1*$^{-/-}$;*Gdf11*$^{-/-}$ and *Foxg1*$^{-/-}$;*Gdf11*$^{+/-}$ mutants, but morphogenesis is still impaired in *Foxg1*$^{-/-}$;*Gdf11*$^{-/-}$ mutants, and even more so in *Foxg1*$^{-/-}$;*Gdf11*$^{+/-}$ animals (Figs 5 and 6). These results stand in marked contrast to the phenotype of *Fst*$^{-/-}$ mice, which exhibit severely defective histogenesis (an extremely thin OE), but relatively normal morphogenesis (see Fig. S1 in the supplementary material). How could excessive *Gdf11* activity disrupt morphogenesis in one situation but not the other?

We believe that the answer lies in the expression pattern of *Foxg1* in the developing OE. As shown in Fig. 2, *Foxg1* is initially found throughout the OE, but soon becomes localized primarily to those areas in which planar expansion of the epithelium is occurring. This implies that Gdf11 levels in most of the OE are normally low enough to permit a constant, steady accumulation of ORNs, driving normal histogenesis. At locations where *Foxg1* is strongly expressed, however, potent inhibition of Gdf11 signaling might allow the tissue to switch into a mode of more dramatic expansion. Recently, we used mathematical modeling to show that the only change needed to convert a tissue that adds cells at a constant rate to one that adds cells at an exponentially increasing rate is adjustment of the 'replication probability' of a stem or transit-amplifying cell to a level above 50% (Lander et al., 2009). As Gdf11 demonstrably lowers INP replication probabilities (Lander et al., 2009; Wu et al., 2003), the idea that a sufficient reduction in *Gdf11* activity could switch the OE into an exponential growth mode is very plausible. In the *Fst*$^{-/-}$ mutant, excessive levels of free extracellular Gdf11 everywhere could account for a reduction in steady-state neurogenesis throughout the OE (and thereby a very thin epithelium), but in regions of *Foxg1* expression, even this higher level of Gdf11 signaling might still be effectively blocked (through the cell autonomous action of Foxg1 on Gdf11 signaling). The result would be that planar expansion, and thus morphogenesis, could proceed normally in the *Fst*$^{-/-}$ mutant. By contrast, in the *Foxg1*$^{-/-}$ OE, unopposed Gdf11 activity would occur everywhere, leading to a failure of both histogenesis and morphogenesis.

In summary, we propose that a major role of Gdf11 is to set a balance between the proliferation and differentiation of progenitor cells, whereas the primary role of Foxg1 is to tip that balance in favor of tissue expansion. A schematic depiction of the balancing act between *Gdf11* and *Foxg1* activities is presented in Fig. 10. It will be interesting to see whether the model of *Foxg1* action through regulation of TGFβ family signaling applies to the OE only, or to other developing neural structures as well. Although *Foxg1* clearly does not act through *Gdf11* in the cerebral cortex (Fig. 9), a potential role for other TGFβ family ligands cannot be ruled out. Alternatively, it may be that, in some neural structures, the positive regulation of pro-neurogenic signals, such as FGFs, is of greater importance than the negative regulation of anti-neurogenic ones.

We thank members of the Calof laboratory for critical comments on the manuscript and Mr Dan L. Phan and Ms Michelle Hoang for technical support. We thank Drs Jean Hebert and Susan McConnell for providing *Foxg1*^{cre} mice, and Dr Martin Matzuk for providing the *Fst* probe and *Fst*$^{+/-}$ mice. This work was funded by NIH grant DC03583 (to A.L.C.) and P50 GM0-76516 (to A.D.L. and A.L.C.). R.S. is supported by a pre-doctoral supplement to NIH grant 1P01-HD052860 (sub2, to A.D.L. and A.L.C.). Deposited in PMC for release after 12 months.

Supplementary material

Supplementary material for this article is available at http://dev.biologists.org/cgi/content/full/136/9/1453/DC1

References

Astic, L., Pellier-Monnin, V., Saucier, D., Charrier, C. and Mehlen, P. (2002). Expression of netrin-1 and netrin-1 receptor, DCC, in the rat olfactory nerve pathway during development and axonal regeneration. *Neuroscience* **109**, 643-656.

Barthels, D., Santoni, M. J., Wille, W., Ruppert, C., Chaix, J. C., Hirsch, M. R., Fontecilla-Camps, J. C. and Goridis, C. (1987). Isolation and nucleotide sequence of mouse NCAM cDNA that codes for a Mr 79,000 polypeptide without a membrane-spanning region. *EMBO J.* **6**, 907-914.

Beites, C. L., Kawauchi, S., Crocker, C. E. and Calof, A. L. (2005). Identification and molecular regulation of neural stem cells in the olfactory epithelium. *Exp. Cell Res.* **306**, 309-316.

Calof, A. L. and Chikaraishi, D. M. (1989). Analysis of neurogenesis in a mammalian neuroepithelium: proliferation and differentiation of an olfactory neuron precursor *in vitro*. *Neuron* **3**, 115-127.

Calof, A. L., Bonnin, A., Crocker, C., Kawauchi, S., Murray, R. C., Shou, J. and Wu, H. H. (2002). Progenitor cells of the olfactory receptor neuron lineage. *Microsc. Res. Tech.* **58**, 176-188.

Carlsson, P. and Mahlapuu, M. (2002). Forkhead transcription factors: key players in development and metabolism. *Dev. Biol.* **250**, 1-23.

Cau, E., Gradwohl, G., Fode, C. and Guillemot, F. (1997). Mash1 activates a cascade of bHLH regulators in olfactory neuron progenitors. *Development* **124**, 1611-1621.

Chen, Y. and Schier, A. F. (2002). Lefty proteins are long-range inhibitors of squint-mediated nodal signaling. *Curr. Biol.* **12**, 2124-2128.

Cuschieri, A. and Bannister, L. H. (1975a). The development of the olfactory mucosa in the mouse: electron microscopy. *J. Anat.* **119**, 471-498.

Cuschieri, A. and Bannister, L. H. (1975b). The development of the olfactory mucosa in the mouse: light microscopy. *J. Anat.* **119**, 277-286.

DeHamer, M. K., Guevara, J. L., Hannon, K., Olwin, B. B. and Calof, A. L. (1994). Genesis of olfactory receptor neurons *in vitro*: regulation of progenitor cell divisions by fibroblast growth factors. *Neuron* **13**, 1083-1097.

Dou, C., Lee, J., Liu, B., Liu, F., Massague, J., Xuan, S. and Lai, E. (2000). BF-1 interferes with transforming growth factor beta signaling by associating with Smad partners. *Mol. Cell. Biol.* **20**, 6201-6211.

Duggan, C. D., Demaria, S., Baudhuin, A., Stafford, D. and Ngai, J. (2008). Foxg1 is required for development of the vertebrate olfactory system. *J. Neurosci.* **28**, 5229-5239.

Dunn, N. R., Winnier, G. E., Hargett, L. K., Schrick, J. J., Fogo, A. B. and Hogan, B. L. (1997). Haploinsufficient phenotypes in Bmp4 heterozygous null mice and modification by mutations in Gli3 and Alx4. *Dev. Biol.* **188**, 235-247.

Eagleson, K. L., Schlueter McFadyen-Ketchum, L. J., Ahrens, E. T., Mills, P. H., Does, M. D., Nickols, J. and Levitt, P. (2007). Disruption of Foxg1 expression by knock-in of cre recombinase: effects on the development of the mouse telencephalon. *Neuroscience* **148**, 385-399.

Eldar, A., Dorfman, R., Weiss, D., Ashe, H., Shilo, B. Z. and Barkai, N. (2002). Robustness of the BMP morphogen gradient in Drosophila embryonic patterning. *Nature* **419**, 304-308.

Forbes, D., Jackman, M., Bishop, A., Thomas, M., Kambadur, R. and Sharma, M. (2006). Myostatin auto-regulates its expression by feedback loop through Smad7 dependent mechanism. *J. Cell Physiol.* **206**, 264-272.

Gamer, L. W., Cox, K. A., Small, C. and Rosen, V. (2001). Gdf11 is a negative regulator of chondrogenesis and myogenesis in the developing chick limb. *Dev. Biol.* **229**, 407-420.

Glantz, S. A. (2005). *Primer of Biostatistics*. New York: McGraw-Hill.

Gomis, R. R., Alarcon, C., Nadal, C., Van Poznak, C. and Massague, J. (2006). C/EBPbeta at the core of the TGFbeta cytostatic response and its evasion in metastatic breast cancer cells. *Cancer Cell* **10**, 203-214.

Guillemot, F. and Joyner, A. L. (1993). Dynamic expression of the murine Achaete-Scute homologue Mash-1 in the developing nervous system. *Mech. Dev.* **42**, 171-185.

Hanashima, C., Shen, L., Li, S. C. and Lai, E. (2002). Brain factor-1 controls the proliferation and differentiation of neocortical progenitor cells through independent mechanisms. *J. Neurosci.* **22**, 6526-6536.

Hanashima, C., Li, S. C., Shen, L., Lai, E. and Fishell, G. (2004). Foxg1 suppresses early cortical cell fate. *Science* **303**, 56-59.

Hanashima, C., Fernandes, M., Hebert, J. M. and Fishell, G. (2007). The role of Foxg1 and dorsal midline signaling in the generation of Cajal-Retzius subtypes. *J. Neurosci.* **27**, 11103-11111.

Hatini, V., Ye, X., Balas, G. and Lai, E. (1999). Dynamics of placodal lineage development revealed by targeted transgene expression. *Dev. Dyn.* **215**, 332-343.

Hebert, J. M. and McConnell, S. K. (2000). Targeting of cre to the Foxg1 (BF-1) locus mediates loxP recombination in the telencephalon and other developing head structures. *Dev. Biol.* **222**, 296-306.
Hebert, J. M. and Fishell, G. (2008). The genetics of early telencephalon patterning: some assembly required. *Nat. Rev. Neurosci.* **9**, 678-685.
Kastner, A., Moyse, E., Bauer, S., Jourdan, F. and Brun, G. (2000). Unusual regulation of cyclin D1 and cyclin-dependent kinases cdk2 and cdk4 during in vivo mitotic stimulation of olfactory neuron progenitors in adult mouse. *J. Neurochem.* **74**, 2343-2349.
Kawauchi, S., Beites, C. L., Crocker, C. E., Wu, H. H., Bonnin, A., Murray, R. and Calof, A. L. (2004). Molecular signals regulating proliferation of stem and progenitor cells in mouse olfactory epithelium. *Dev. Neurosci.* **26**, 166-180.
Kawauchi, S., Shou, J., Santos, R., Hebert, J. M., McConnell, S. K., Mason, I. and Calof, A. L. (2005). Fgf8 expression defines a morphogenetic center required for olfactory neurogenesis and nasal cavity development in the mouse. *Development* **132**, 5211-5223.
Kim, J., Wu, H.-H., Lander, A. D., Lyons, K. M., Matzuk, M. M. and Calof, A. L. (2005). GDF11 controls the timing of progenitor cell competence in developing retina. *Science* **308**, 1927-1930.
Lander, A. D., Gokoffski, K. K., Wan, F. Y. M., Nie, Q. and Calof, A. L. (2009). Cell Lineages and the Logic of Proliferative Control. *PLoS Biol.* **7**, e1000015.
Lawson, K. A., Dunn, N. R., Roelen, B. A., Zeinstra, L. M., Davis, A. M., Wright, C. V., Korving, J. P. and Hogan, B. L. (1999). Bmp4 is required for the generation of primordial germ cells in the mouse embryo. *Genes Dev.* **13**, 424-436.
Legrier, M. E., Ducray, A., Propper, A., Chao, M. and Kastner, A. (2001). Cell cycle regulation during mouse olfactory neurogenesis. *Cell Growth Differ.* **12**, 591-601.
Lewandoski, M., Meyers, E. N. and Martin, G. R. (1997). Analysis of Fgf8 gene function in vertebrate development. *Cold Spring Harb. Symp. Quant. Biol.* **62**, 159-168.
Ma, Q., Fode, C., Guillemot, F. and Anderson, D. J. (1999). Neurogenin1 and neurogenin2 control two distinct waves of neurogenesis in developing dorsal root ganglia. *Genes Dev.* **13**, 1717-1728.
Mallamaci, A., Di Blas, E., Briata, P., Boncinelli, E. and Corte, G. (1996). OTX2 homeoprotein in the developing central nervous system and migratory cells of the olfactory area. *Mech. Dev.* **58**, 165-178.
Martynoga, B., Morrison, H., Price, D. J. and Mason, J. O. (2005). Foxg1 is required for specification of ventral telencephalon and region-specific regulation of dorsal telencephalic precursor proliferation and apoptosis. *Dev. Biol.* **283**, 113-127.
Massague, J. (2000). How cells read TGF-beta signals. *Nat. Rev. Mol. Cell Biol.* **1**, 169-178.
Massague, J. and Gomis, R. R. (2006). The logic of TGFbeta signaling. *FEBS Lett.* **580**, 2811-2820.
Moustakas, A., Souchelnytskyi, S. and Heldin, C. H. (2001). Smad regulation in TGF-beta signal transduction. *J. Cell Sci.* **114**, 4359-4369.
Mumm, J. S., Shou, J. and Calof, A. L. (1996). Colony-forming progenitors from mouse olfactory epithelium: evidence for feedback regulation of neuron production. *Proc. Natl. Acad. Sci. USA* **93**, 11167-11172.
Murray, R. C., Navi, D., Fesenko, J., Lander, A. D. and Calof, A. L. (2003). Widespread defects in the primary olfactory pathway caused by loss of Mash1 function. *J. Neurosci.* **23**, 1769-1780.
Muzio, L. and Mallamaci, A. (2005). Foxg1 confines Cajal-Retzius neuronogenesis and hippocampal morphogenesis to the dorsomedial pallium. *J. Neurosci.* **25**, 4435-4441.
Nakamura, T., Takio, K., Eto, Y., Shibai, H., Titani, K. and Sugino, H. (1990). Activin-binding protein from rat ovary is follistatin. *Science* **247**, 836-838.
Nakashima, M., Toyono, T., Akamine, A. and Joyner, A. (1999). Expression of growth/differentiation factor 11, a new member of the BMP/TGFbeta superfamily during mouse embryogenesis. *Mech. Dev.* **80**, 185-189.
Newfeld, S. J., Wisotzkey, R. G. and Kumar, S. (1999). Molecular evolution of a developmental pathway: phylogenetic analyses of transforming growth factor-beta family ligands, receptors and Smad signal transducers. *Genetics* **152**, 783-795.
Nguyen, T. T., Cho, K., Stratton, S. A. and Barton, M. C. (2005). Transcription factor interactions and chromatin modifications associated with p53-mediated, developmental repression of the alpha-fetoprotein gene. *Mol. Cell. Biol.* **25**, 2147-2157.
Nomura, T., Ueyama, T., Ashihara, E., Tateishi, K., Asada, S., Nakajima, N., Isodono, K., Takahashi, T., Matsubara, H. and Oh, H. (2008). Skeletal muscle-derived progenitors capable of differentiating into cardiomyocytes proliferate through myostatin-independent TGF-beta family signaling. *Biochem. Biophys. Res. Commun.* **365**, 863-869.
Pauley, S., Lai, E. and Fritzsch, B. (2006). Foxg1 is required for morphogenesis and histogenesis of the mammalian inner ear. *Dev. Dyn.* **235**, 2470-2482.
Pratt, T., Tian, N. M., Simpson, T. I., Mason, J. O. and Price, D. J. (2004). The winged helix transcription factor Foxg1 facilitates retinal ganglion cell axon crossing of the ventral midline in the mouse. *Development* **131**, 3773-3784.
Regad, T., Roth, M., Bredenkamp, N., Illing, N. and Papalopulu, N. (2007). The neural progenitor-specifying activity of FoxG1 is antagonistically regulated by CKI and FGF. *Nat. Cell Biol.* **9**, 531-540.
Rodriguez, C., Huang, L. J., Son, J. K., McKee, A., Xiao, Z. and Lodish, H. F. (2001). Functional cloning of the proto-oncogene brain factor-1 (BF-1) as a Smad-binding antagonist of transforming growth factor-beta signaling. *J. Biol. Chem.* **276**, 30224-30230.
Schneyer, A. L., Rzucidlo, D. A., Sluss, P. M. and Crowley, W. F., Jr (1994). Characterization of unique binding kinetics of follistatin and activin or inhibin in serum. *Endocrinology* **135**, 667-674.
Schneyer, A. L., Sidis, Y., Gulati, A., Sun, J. L., Keutmann, H. and Krasney, P. A. (2008). Differential antagonism of activin, myostatin and GDF11 by wild type and mutant follistatin. *Endocrinology* **149**, 4589-4595.
Seoane, J., Le H. V., Shen, L., Anderson, S. A. and Massague, J. (2004). Integration of Smad and forkhead pathways in the control of neuroepithelial and glioblastoma cell proliferation. *Cell* **117**, 211-223.
Shimamura, K. and Rubenstein, J. L. (1997). Inductive interactions direct early regionalization of the mouse forebrain. *Development* **124**, 2709-2718.
Smart, I. H. (1971). Location and orientation of mitotic figures in the developing mouse olfactory epithelium. *J. Anat.* **109**, 243-251.
Storm, E. E., Garel, S., Borello, U., Hebert, J. M., Martinez, S., McConnell, S. K., Martin, G. R. and Rubenstein, J. L. (2006). Dose-dependent functions of Fgf8 in regulating telencephalic patterning centers. *Development* **133**, 1831-1844.
Sutherland, D. J., Li, M., Liu, X. Q., Stefancsik, R. and Raftery, L. A. (2003). Stepwise formation of a SMAD activity gradient during dorsal-ventral patterning of the Drosophila embryo. *Development* **130**, 5705-5716.
Tsuchida, K., Nakatani, M., Uezumi, A., Murakami, T. and Cui, X. (2007). Signal transduction pathway through activin receptors as a therapeutic target of musculoskeletal diseases and cancer. *Endocr. J.* **55**, 11-21.
Wu, H. H., Ivkovic, S., Murray, R. C., Jaramillo, S., Lyons, K. M., Johnson, J. E. and Calof, A. L. (2003). Autoregulation of neurogenesis by GDF11. *Neuron* **37**, 197-207.
Xuan, S., Baptista, C. A., Balas, G., Tao, W., Soares, V. C. and Lai, E. (1995). Winged helix transcription factor BF-1 is essential for the development of the cerebral hemispheres. *Neuron* **14**, 1141-1152.